Peak load reduction and load shaping in HVAC and refrigeration systems in commercial buildings by using a novel lightweight dynamic priority-based control strategy\*

Christopher Winstead, Mahabir Bhandari\*, James Nutaro, Teja Kuruganti Oak Ridge National Laboratory, One Bethel Valley Road, Oak Ridge, TN 37831, USA

\* Correspondence: bhandarims@ornl.gov; Tel.: +1-865-574-0989

### **ABSTRACT**

Reducing peak power demand in a building can reduce electricity expenses for the building owner and contribute to the efficiency and reliability of the electrical power grid. For the building owner, reduced expenses come from the reduction or elimination of peak power charges on electricity bills. For the power system operator, reducing peak power demand leads to a more predictable load profile and reduces stress on the electric grid system. We present a computationally inexpensive, dynamic, and retrofit-deployable control strategy to effect peak load reduction and load shaping. The effectiveness of the control strategy is examined in a simulation with 80 airconditioning units and 40 refrigeration units. The results show that a peak demand reduction of 60 kW can be achieved relative to peak demand in a typical set point—based approach. The proposed strategy was deployed in a gymnasium building with four rooftop HVAC units, where it showed over 15% peak demand (kW) reduction savings while maintaining or lowering energy consumption (in kilowatt-hours) relative to the set point—based thermostat controls.

<sup>\*</sup>This manuscript has been authored by UT-Battelle, LLC, under contract DE-AC05-00OR22725 with the US Department of Energy (DOE). The US government retains and the publisher, by accepting the article for publication, acknowledges that the US government retains a nonexclusive, paid-up, irrevocable, worldwide license to publish or reproduce the published form of this manuscript, or allow others to do so, for US government purposes. DOE will provide public access to these results of federally sponsored research in accordance with the DOE Public Access Plan (<a href="http://energy.gov/downloads/doe-public-access-plan">http://energy.gov/downloads/doe-public-access-plan</a>).

Keywords: demand-side management; load shaping; peak demand reduction; Priority-based control; transactive control; IoT

# Nomenclature

CBC COIN-OR Branch and Cut

DR demand response

HVAC heating, ventilating, and air conditioning

kWh kilowatt hours

MPC model predictive control

MWh megawatt hours

PBC priority-based control

PJ petajoules  $(J \times 10^{16})$ 

RTU rooftop units

TBtu trillion British thermal units

TCL thermostatically controlled loads

### 1. Introduction

Interest in the potential of thermostatically controlled loads (TCLs) as thermal storage started in the early 1980s [1]. Owing to their inherently large thermal storage capabilities, TCLs such as heating, ventilating, and air-conditioning (HVAC) systems, refrigerators, and water heaters can provide ancillary service to electric utilities by taking advantage of their flexible power requirements [2]. In the United States, TCLs account for 48% of the electricity consumed in commercial buildings [3], with grocery and convenience stores making up a large fraction of this

energy use. A survey of food sales buildings [4], which encompass grocery stores, convenience stores, corner stores, gas station stores, and superstores, found that they consume 6.33 PJ (6 TBtu) of electricity for cooling and 125.55 PJ (119 TBtu) for refrigeration each year. There are 176,700 food sales buildings in the United States, and their heating and cooling accounts for 2% of the electricity used in the country. These buildings, with their significant air-conditioning and refrigeration needs, are ideal candidates for providing electric utilities with peak demand—shaving and load-shaping services.

Despite their huge consumption of electricity, grocery stores are relatively underutilized candidates in most demand response (DR) programs, which have largely focused on residential buildings. The Cadmus Group analyzed the regional distribution of commercial buildings and their end uses in the Pacific Northwest and found that grocery stores were open for business an average of 113 hours per week and consumed 4.1 million MWh of electric power in 2007 [5]. A case study by the California Energy Commission of 300 Albertsons supermarkets reported that 7.5 MW of peak demand could be shed using sales lighting and anti-sweat door heaters [6]. Field testing and simulations of using low-temperature refrigeration systems in supermarkets for demand reduction provided an estimate of how much power may be shed in the northwestern United States [7]. The simulations in this study showed that demand savings of 15 to 20 kW are available for 1.5 hours for a typical store without precooling, and for about 2.5 hours with precooling, using only the low-temperature non-ice-cream cases.

Operators of commercial buildings have an incentive to participate in DR programs, particularly with respect to reducing peak demand charges. A survey [8] undertaken by the National Renewable Energy Laboratory determined these charges can range on average from about \$5.00 to \$22.00 per month depending on the utility. This incentive, though small, could be

sufficient to create widespread adoption of a sufficiently low-cost retrofit technology for peak demand reduction and load shaping.

Prior work on model predictive control (MPC) for demand shaping relied on a forecast of the building temperature and energy demand to devise an optimal schedule for electrical appliances; this section provides a review on related work. Although effective in a research setting, MPC can be impractical in practice, particularly in retrofit deployment scenarios in which minimal information about building parameters is available and there is a limited or non-existent sensor infrastructure. The transient nature of a building's condition requires frequent model recalibration and thus a shortened forecasting horizon, which reduces the effectiveness of the MPC. Additionally, MPC is often computationally burdensome, which hampers both scalability and the ability to deploy controllers on inexpensive devices.

To overcome these limitations, we introduce priority-based control (PBC), which is a computationally inexpensive control strategy for achieving peak load reduction. With this strategy, devices assess local deviations from a set point and relay this information to a scheduler. The scheduler then allows a subset of the devices to run, based on which are furthest from their set point. Devices that exceed a certain distance from the set point are required to run to ensure occupant comfort.

In prior work, we described conditions under which performance guarantees can be made when using PBC to track a load shape while maintaining temperature constraints; see ref. [9]. Significantly, the guarantee for the load shape does not depend on the availability of a valid model of the equipment being controlled, and a concomitant statement regarding temperature regulation requires only the most rudimentary assumptions. Guarantees regarding load tracking and temperature for MPC would necessarily make strong assumptions about the validity of the

underlying model. Moreover, the computational overhead of the proposed PBC is drastically reduced relative to MPC, as PBC does not require any forecasting for optimization; the only computational burden is sorting the device list in order of priority. Nonetheless, we demonstrate that this strategy is effective in a small building where the control strategy was deployed, and we demonstrate the potential for scalability via simulation.

### 2. Related Work

Callaway [10] proposed a method for manipulating temperature set points in a large population of TCLs to control power without compromising the thermal comfort of individual users. Kundu et al. [11] adopted a global temperature set point offset as an output signal of a feedback controller approach and designed a linear quadratic regulator to enable aggregate power to track a reference signal that exhibits step, ramp, and sinusoidal variations. A statistical approach was proposed to describe a cluster of TCLs as a system of coupled Fokker-Planck equations [12]. A general load modeling and control framework with flexibility in terms of parameter and states estimation and control design was introduced using a linear time-invariant representation of a population of 1,000 TCLs [13]. The accuracy of the state-queuing model used to characterize the dynamics of aggregated TCLs was investigated using an equivalent thermal parameter model [14]. Bao et al. [15] proposed an analysis of state-queuing model accuracy and improvement for TCLs. Aggregation of the continuous temperature dynamics of a homogenous population of TCLs was represented by a finite-space stochastic dynamic model that was extended to a heterogenous population of TCLs [16]. An analytical model was developed to aggregate the power response of a homogeneous population of TCLs to uniform variation of all TCL set points [11]. For the cases in which the measured state information was not available in real time, a load-following model using TCLs was discussed using a Markov chain model and Kalman filtering [17]. The same

modeling framework was used [13] with a focus on TCLs that are heterogenous in all TCL parameters, not just thermal capacitance. In the study, load was controlled with very little information with regard to the performance.

On/off operation to manage large populations of domestic refrigerators for DR was performed using ref. [18]. To capture the behavior of the population, a temperature distribution model based on Fokker-Planck partial differential equations was used. An open-loop MPC using a broadcast strategy with two switching-fraction signals (on/off) was used to track power reference. Field experiments for domestic refrigerators as TCLs (25 refrigerators were used in the experiments) are documented in refs. [19] [20]. The simple controller used in the experiments switched the refrigerators that meet the temperature limits one-by-one until the power limit was reached. The order of the refrigerators selected depended on the longest time a refrigerator could be on without violating the temperature limits. Refrigerators were also used to study applicability of domestic TCLs for load shifting in a low-voltage distribution grid [21]. In the study, an evaluation of the potential for load shifting by TCLs was performed with two 1-week-long experiments with real-time measurements from 10 real households using adaptive load prediction. A reduction in total threshold crossing time by 37.48% with energy reduction by 17 kWh was achieved with an increase in cold chamber temperature of 1.7°C.

Two control logics using heterogenous TCLs as frequency-controlled reserves were simulated [22]. One of the control strategies tripped the load based on the system frequency, while the other controlled the temperature set points. A two-level scheduling method was used to schedule flexible TCLs with renewable energy to arbitrage in the intraday electricity market [23]. The top level used an MPC optimization, and the bottom level used temperature priority list control. The proposed method reduced the imbalance peak and showed performance degradation

with increasing heterogeneity or uncertainty in the forecast. A temperature priority list method to prioritize each air conditioner load based on how close it was to being turned on or off was used in ref. [24]. The study found that the number of HVAC units needed to provide a ±1 MW load-balancing service varied significantly with baseline settings, high and low temperature settings, and outdoor temperatures. This control scheme was further expanded to include a simplified forecaster model and peak-shaving and load-shifting capabilities [25]. A study to model the aggregate flexibility offered by a collection of TCLs (1,000 diverse air conditioners) as a stochastic battery with dissipation has been proposed [26]. The power limits and energy capacity of this battery model were characterized in terms of TCL parameters and variables such as ambient temperature and set point temperature. A priority-stack—based control of TCLs using a direct load control architecture was used to track the control signal supplied by the system operator and showed excellent tracking performance and good robustness.

A simulation study used for energy cost optimization and balancing service for a supermarket refrigeration system using MPC is discussed in ref. [27]. The study focused on the development of a simulation benchmark using MPC for cost optimization and balancing services of a small set of loads. Control strategies for the aggregation of a portfolio of supermarkets toward the electricity balancing market were investigated [28]. A simple interface between the supermarkets and an aggregator was proposed by characterizing each supermarket by two distinct operation modes, "on" and "off," or all of the supermarkets collectively as the "storage mode state." O'Connell et al. [29] reported a concept of asymmetric block offers for flexible loads to describe the load shifting ability of flexible electrical loads in a manner suitable for existing power system dispatch frameworks. The case studies in this work demonstrated that DR from supermarket refrigeration systems, as described using a limited set of block offers, can achieve

substantial cost savings in the procurement of regulating power. A laboratory experimental and analytical study was conducted to determine the potential of a supermarket display case to be used for energy storage [30]. A one-dimensional transient heat conduction analysis was used to validate the experimental results. Fricke et al. concluded that using an advanced controller that can respond to a utility signal in a refrigeration system could enable demand shifting with minimal impact.

## 3. Methods and Control Strategy Formulation

The proposed control strategy is a supervisory strategy for limiting the peak power demand of small and medium commercial buildings, including grocery and convenience stores, while still meeting the comfort requirements of the occupants. First described in ref. [31], the objective of this supervisory control strategy is never to operate more than N loads while satisfying equipment limits on acceptable operation, and to exceed N only when these constraints cannot otherwise be satisfied. This is accomplished by assigning priority points to each device based on its deviation from a set point. In a heating and cooling application, priority points are calculated by discretizing the distance between the current temperature and the device's set point. One such method of computing the priority points is

$$p = egin{cases} ceil\left(rac{T-S}{\Delta}
ight) & if \ 0 < T-S < 1 \ 0 & T \leq S \ rac{d_{max}}{\Delta} & T-S \geq d_{max} \end{cases},$$

where T is the current temperature, S is the set point,  $d_{max}$  is the maximum allowable deviation from the set point, and  $\Delta$  is the granularity of the discretization. When  $T - S > d_{max}$ , the priority is  $\frac{d_{max}}{\Delta}$ , otherwise known as maximum priority  $(p_{max})$ . This formulation allows for different operating ranges and levels of granularity depending on the application. The customization of operating range and granularity follows the degree to which an application requires precision in

data. The finer data precision, or the larger the number of participating units, the more sensitive levels of priority required to effectively sort the list of devices.

The formulation is lightweight in terms of required computation, as no model-based optimization is required. The largest computational demand is the time required to sort the list in order of priority. Furthermore, the control strategy is generally extensible to a heterogenous set of devices, as all devices interact with the scheduler by exchanging priority points. Specifically, a device need only have a means to translate the difference between its current state and the desired state into a priority, which hides device idiosyncrasies from the PBC.

The control strategy formulation is principally derived from three core tenets.

- 1. The desired state of a device is determined at a local level. This local determination is communicated to the scheduler in the form of priority points.
- 2. A device does not unilaterally change state.
- 3. There is some number N of devices that can be simultaneously activated while still reducing peak demand. This has been shown in ref. [31].

From these principles, we derive the simple workflow for demand reduction, which is shown in Fig. 1.

## **Scheduler Workflow**

While true:

For device in device\_list:

Log equipment state

Compute priority

Sort device\_list by priority

For device in device\_list:

If priority == max priority:

Activate device

Elif number activated devices < max allowed activated devices:

Activate device

Elif number activated devices > max allowed activated device:

Deactivate device

Elif priority == minimum priority:

Deactivate device

Dispatch command

**Fig. 1.** The algorithm for peak demand reduction as pseudocode. There are three primary steps in the algorithm: query the equipment state, sort the equipment by priority, and dispatch the command.

At the start of each period in the workflow, data are gathered from the devices. These data are the current operating state, desired operating state, activation eligibility, and priority. Activation eligibility is determined by some minimum cycle timer to avoid short cycling of the device. The algorithm first determines the devices that are eligible for activation. Those that are eligible are sorted in order of descending priority. Traversing this sorted list, the algorithm activates devices until N are active. From then on, all remaining devices are deactivated. Two constraints exist in this formulation. First, a device that is at maximal priority must be activated regardless of the number of concurrently activated devices. This constraint ensures that the temperature regulated by a particular device stays inside an acceptable region. Second, a device at its minimal priority

must be deactivated. Because the algorithm does not have an optimization step, the computational footprint is small, allowing for quick action and reaction.

This algorithm can be augmented to track a general electrical load shape. This reformulation requires information concerning the power consumption of the device. Rather than seeking to restrict the number of active loads to N at all times, the algorithm uses this information to activate loads sufficient to meet the targeted demand. Furthermore, by instituting a comfort band rather than a strict set point, the maximum and minimum priorities can be relaxed to access a wider pool of available assets. This change allows for precooling to shift electrical demand via an approach that can be used to better exploit time-of-use rates, for instance.

The load-shaping algorithm begins similarly to the algorithm for peak load reduction, with the computation of a set of priorities based on device set points and deadbands. From there, the steps are as shown in Fig. 2.

# **Load Shaping Workflow**

While sum(power) != desired power:

For device in device list:

Compute device priorities

Sort device\_list by priority:

For device in device\_list:

If device is maximum priority:

Activate device

Elif desired power level not reached:

Activate device

Elif desired power level reached:

Deactivate device

Elif device is minimum priority:

Deactivate device

If sum(power) within threshold of desired load value:

Dispatch command to devices

Break

Else:

Widen maximum/minimum priorities

If priority expansion maximum reached:

Dispatch command to devices

Break

Continue

**Fig. 2.** The PBC algorithm extended to more generalized load shaping. The maximum and minimum priorities can be expanded to accept or refuse more devices until a desired power level is reached.

# Scalability

The scalability of the PBC formulation is limited chiefly by the ability to sort increasing numbers of devices. Sorting is a well-studied computational problem, and many options exist for quick and efficient sorting. This is in contrast to MPC or machine learning—based control, which often require large amounts of historical data to tune or train representative models. These models are then used in numerical calculations that can be very computationally demanding. Furthermore,

as new assets are introduced into the control, the optimization problem for a model-based control becomes increasingly complex, requiring either more time to solve or more computational power.

As an example, the COIN-OR Branch and Cut Solver (CBC) is a commonly used open-source solver for mixed integer programming problems such as those seen in HVAC control [32]. However, ref. [33] shows that as problem complexity increases, so does solution time. This scaling is an obstacle that is not shared by PBC.

The small computational cost of PBC offers another advantage over model-based controls by allowing for a finer granularity of action in time. In particular, by having a very large number of assets whose priorities are sampled at a high rate, we can approximate continuous load regulation. A very large number of assets reduces the impact that short-cycle restrictions have on load shaping by ensuring that a majority may be switched at any time. Indeed, if a sufficient number of devices are not in a short cycle lock at any particular time, the PBC can quickly adjust the set of active devices to obtain a desired response. This type of fine-grained action in time opens the novel possibility of a frequency or voltage regulation service acting over large areas.

A potential impediment to scalability is homogenization of priorities across the different assets. That is, if priorities began to move together so that all assets were reaching maximum or minimum priority concurrently, the load shaping capability would be significantly reduced. However, given an increasingly diverse set of thermal behaviors—both in terms of thermal characteristics such as envelope insulation and usage patterns, and driving factors such as solar heating and internal heat loads—this type of synchronized movement of priorities becomes increasingly unlikely. Allowing for a wider deadband to facilitate differences in temperature can further mitigate any potential synchronicity.

# 4. Simulation and Physical Demonstration

The performance of PBC was examined in two separate experiments. The first experiment was a simulation in which the PBC managed several HVAC and refrigeration units. The second experiment was a field trial in which the PBC was used to manage four HVAC units in a gymnasium.

### 4.1 Simulation Experiment

We simulated a deployment of the PBC to control 80 HVAC units and 40 refrigeration units. The scheduling algorithm was implemented using Python, as described in Section 4.2. The sensors and actuators in the fielded software (see Section 4.2) were replaced with models to simulate a large-scale deployment. The simulated HVAC units used 5 kW of power when operating, and the refrigeration units used 2 kW. These power ratings were chosen arbitrarily for the purpose of simulation, but they are broadly consistent with the power requirements of actual equipment.

The simulation used statistical models of the equipment, which randomly assign a simple thermal behavior to each item of equipment. This thermal behavior consisted of a negative temperature rate of change when the equipment was active and a positive, time-of-day-dependent temperature rate of change when the equipment was inactive. A baseline rate of change was established, and the specific temperature rates of change were selected at random from 50% to 200% of the baseline for each individual piece of equipment.

The algorithm for peak load reduction includes specific safeguards against the equipment temperature falling out of an acceptable range. Specifically, if the temperature within a refrigerated unit or within an air-conditioned zone exceeds the specified tolerance, then the unit will run

regardless of other considerations. Consequently, the baseline control using set points and the PBC yield similar results for temperature regulation, so we do not consider temperature further here.

Given enough variation in the equipment behavior, the simulation demonstrated that PBC is viable across a wide range of environmental conditions. PBC was compared with set point—deadband control by tracking the aggregated power consumption at each step of the respective simulations. Set point—deadband control was chosen for comparison because it is a common uncoordinated strategy in light commercial buildings. Demonstration of an improvement over this baseline provides a compelling motivation for the proposed control strategy as a retrofit technology targeting these buildings. A comparison of aggregate power consumption is shown in Fig. 3 and the number of active units can be seen in Fig. 4. Both Fig. 3 and Fig. 4 demonstrate that PBC was able to reduce the load peak, resulting in a peak power savings of 46 kW. This was achieved by successfully coordinating the scheduling of the loads so that no more than 60 pieces of equipment were active at any one time.

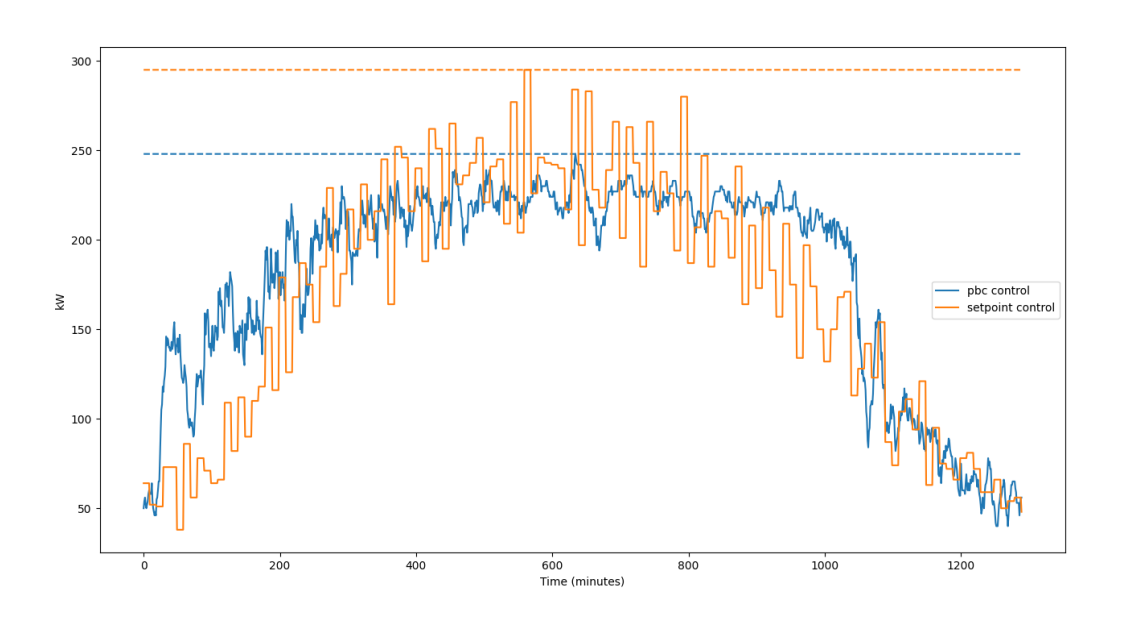


Fig. 3. Simulated power consumption of set point-based control and priority-based control (PBC).

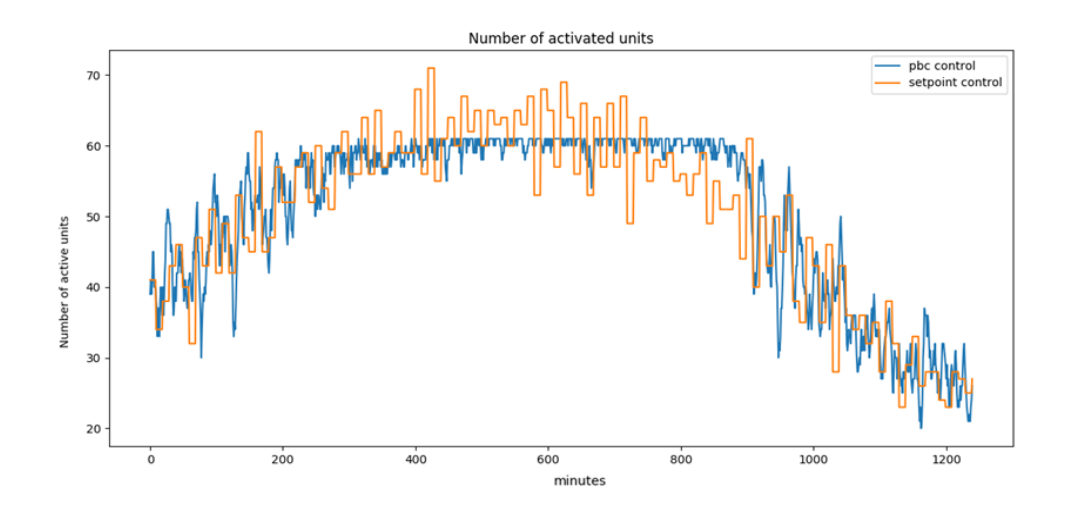
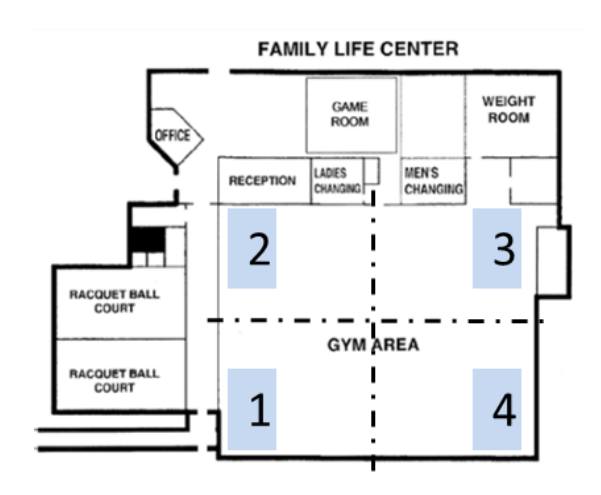


Fig. 4. Simulated number of activated units for set point–based control and priority-based control (PBC).

## 4.2 Physical Demonstration

The initial plan for demonstrating the PBC strategy for HVAC and refrigeration system units could not be accomplished, as delays occurred in recruiting the participating refrigeration stores, implementing the scheduling strategy, and installing measurement equipment. However, a gymnasium in a church building located in Fountain City, Tennessee, USA, which is served by four 5.5 kW (10 ton) rooftop units (RTUs), was available for demonstrating the PBC. The gymnasium is 280 m<sup>2</sup> (3,000 ft<sup>2</sup>) and houses various activities. This physical demonstration covered temperature regulation using the rooftop HVAC units exclusively. The floor plan is shown in Fig. 5. Each HVAC has two cooling stages and two heating stages. For the purposes of this evaluation, heating was disabled.



**Fig. 5.** Gymnasium floor plan with heating, ventilating, and air-conditioning zones; four rooftop units serve the individual zones indicated as 1–4.

For each zone, the legacy thermostat was removed and replaced with a new thermostat consisting of a Raspberry Pi 2 mounted on a shield. Each thermostat carried a temperature sensor, a humidity sensor, and electronic relays to actuate the associated HVAC. Communication between the thermostats was accomplished using on-site Wi-Fi. Each thermostat carried the Volttron software platform [34] and deployed the PBC algorithm as a series of three Volttron agents. A Volttron central instance provided the interface between the building owner and the software agents. The Volttron central instance was deployed on one of the thermostats used in the installation.

The three agents installed on a thermostat consisted of a thermostat agent, responsible for polling the thermostat's temperature and set point and calculating a priority; a scheduler agent, responsible for coordinating the operation of all loads; and a local agent, which was a stand-alone, independent control that handled thermostat operation in the event of a wireless network outage or other system breakdown. The local algorithm realized a simple set point control in which the first

cooling stage was triggered at T = Setpoint + 0.14°C and the second cooling stage was triggered at T = Setpoint + 1.1°C.

Each thermostat carried its own copy of the scheduler agent as a means to increase robustness in the event that the lead scheduler agent should drop off the network. A leader selection process operated within the thermostat agents to decide which scheduler agent the thermostats should look to for control decisions. To avoid short cycling of the HVAC units, a 10-minute minimum interval between switching between on and off was enforced by the algorithm.

The goal of the PBC was to coordinate the four HVAC units so that the gym remained near the temperature set points while limiting peak demand. The HVAC units had two stages, with the second stage reserved for zones that reached maximum priority. The testing followed a week-on (when PBC was deployed) then week-off (traditional set point control) schedule to compare the PBC and traditional set point–deadband control. The weeks of 7/28–8/3 and 8/18–8/24 were monitored with traditional set point controls (referred to as "uncontrolled"), while the weeks of 8/11–8/17, 8/25–8/31, and 9/15–9/21 were monitored with the PBC strategy (referred to as "controlled"). The results of the uncontrolled and controlled cases are illustrated in Fig. 6–Fig. 8. Fig. 6 shows that the PBC strategy gives the lowest peak demand (13.5 kW) compared with peak demand of 15.8 and 17.5 kW with the traditional control strategy. Similar peak demand reduction is shown in Fig. 7 and Fig. 8.

Attempts were made to control for gymnasium use and weather in comparing the weeks shown. The average daily maximum and median daily maximum temperatures were recorded for each observed time frame. The daily maximum was chosen, as this is the outside influence most likely to trigger a peak demand event. The power measurements were a 30-minute sliding average in accordance with the local rate scheduling for peak demand costs. In the testing area, the local

utility charge for this building class was \$13.89 per kilowatt over 50 kW over a 1-month timeframe. In practice, this rate structure means that a substantial portion of a light commercial building's utility costs could potentially result from peak demand charges.

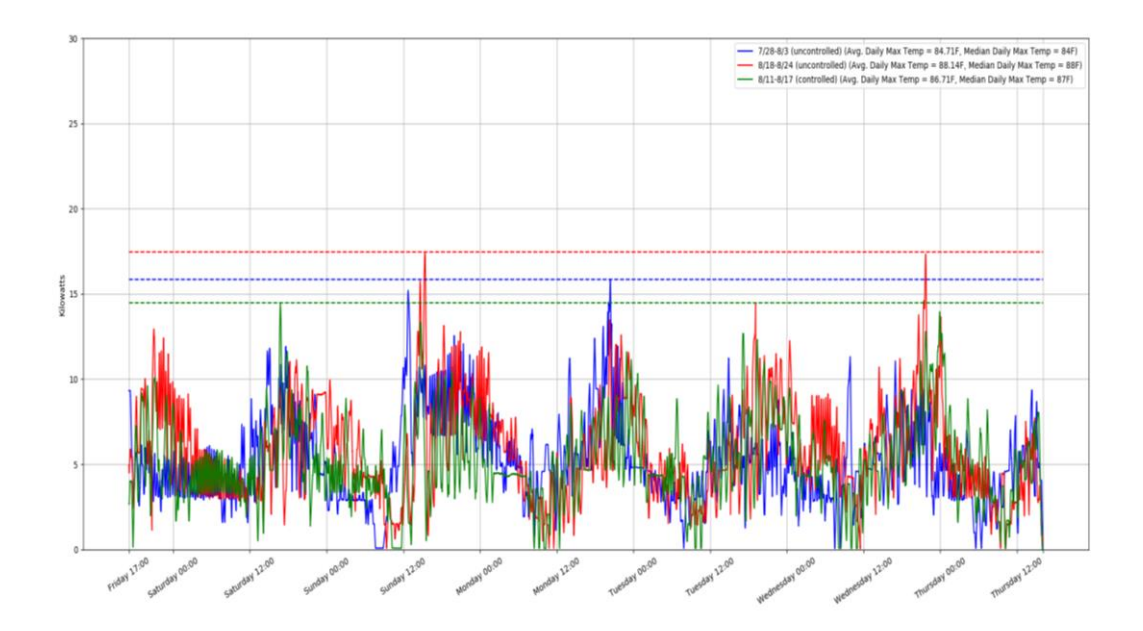


**Fig. 6.** Peak demands for controlled week 8/11-8/17 (green, average daily max temp = 30.4°C, median daily max temp = 30.5°C) and uncontrolled weeks 7/28-8/3 (blue, average daily max temp = 29.3°C, median daily max temp = 28.9°C) and 8/18-8/24 (red, average daily max temp = 31.2°C, median daily max temp = 31.1°C).

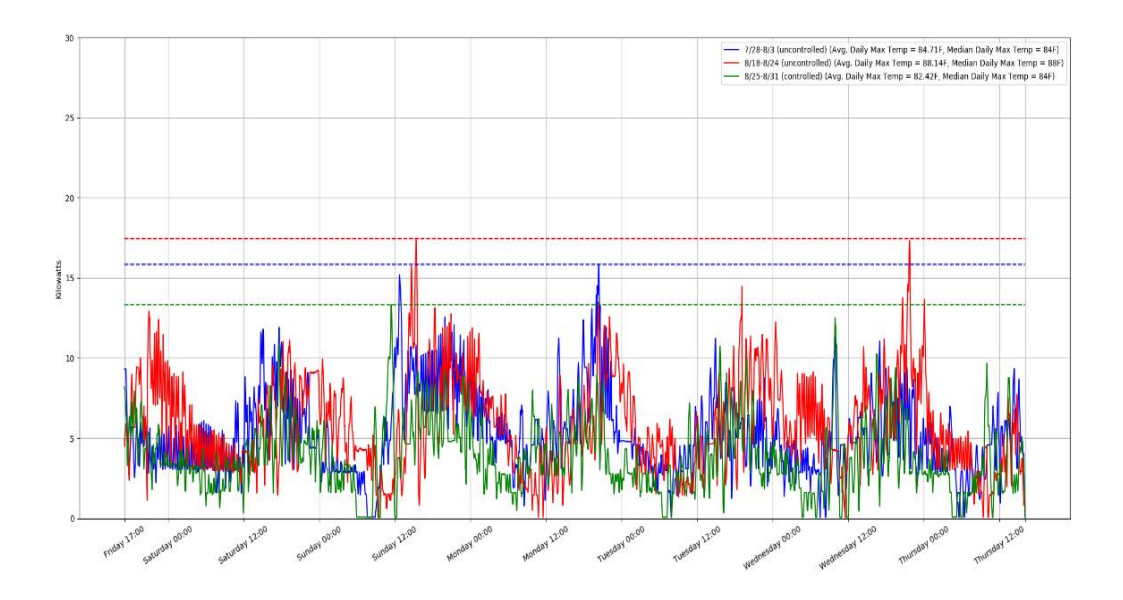


**Fig. 7.** Peak demands for controlled week 8/25-8/31 (green, average daily max temp = 28°C, median daily max temp = 28.9°C) and uncontrolled weeks 7/28-8/3 (blue, average daily max temp = 29.3°C, median daily max temp = 28.9°C) and 8/18-8/24 (red, average daily max temp = 31.2°C, median daily max temp = 31.1°C).

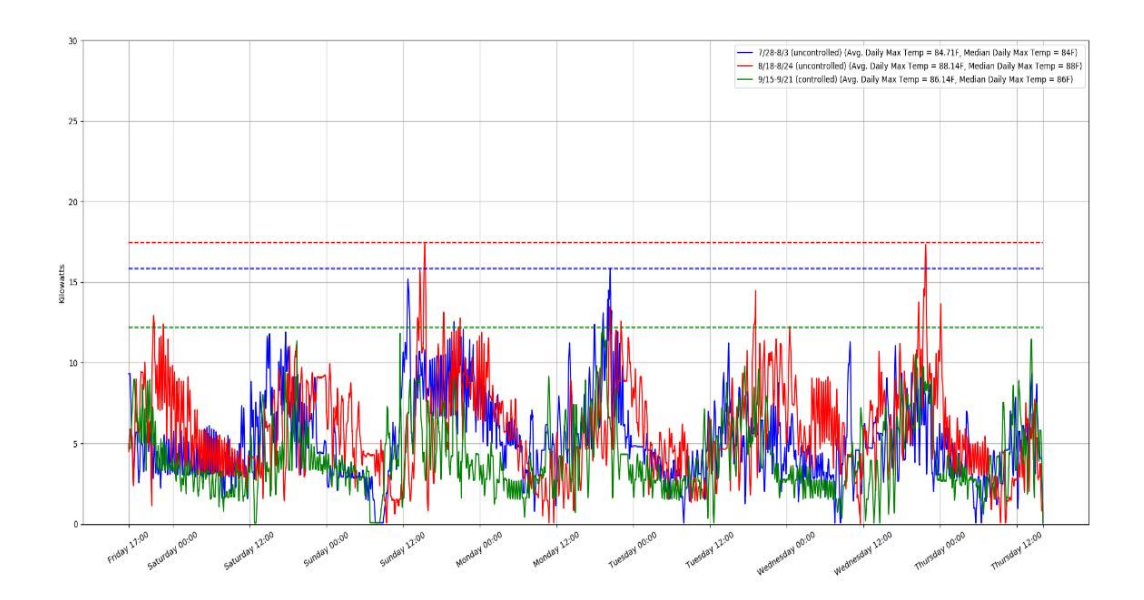


**Fig. 8.** Peak demands for controlled week 9/15-9/21 (**green**, average daily max temp =  $30.1^{\circ}$ C, median daily max temp =  $30^{\circ}$ C) and uncontrolled weeks 7/28-8/3 (**blue**, average daily max temp =  $29.3^{\circ}$ C, median daily max temp =  $28.9^{\circ}$ C) and 8/18-8/24 (**red**, average daily max temp =  $31.2^{\circ}$ C, median daily max temp =  $31.1^{\circ}$ C).

In the observed weeks, PBC resulted in lower peak demand than comparable weeks running traditional set point control. These findings are summarized in Table 1. For example, the table shows that for weeks of similar weather conditions, 7/28–8/3 (uncontrolled) and 8/25–8/31 (controlled), PBC reduced the peak demand by 2.5 kW (15%). Furthermore, the PBC kept the thermal comfort of the zones near dictated set points the vast majority of the time.

As the algorithm's response is ultimately dictated by a set of rules that enforce decisions based on current zone temperatures, the zone temperature is unlikely to escape thermal constraints for a significant amount of time before the deviation is corrected.

In any building control, temperatures must be kept within comfort boundaries as much as possible. Fig. 9, Fig. 10, and Fig. 11 show the temperatures of each of the observed zones. The threshold at which the zone has exceeded the desired thermal zone is denoted by the red "cooling stage 2 activation line." This is the threshold at which the algorithm acts to immediately correct the zone. While the size and thermal momentum of the zones at times led to the temperature

response of the zones not being immediate, the algorithm was largely able to minimize the amount of times the controlled zones were outside the boundary.

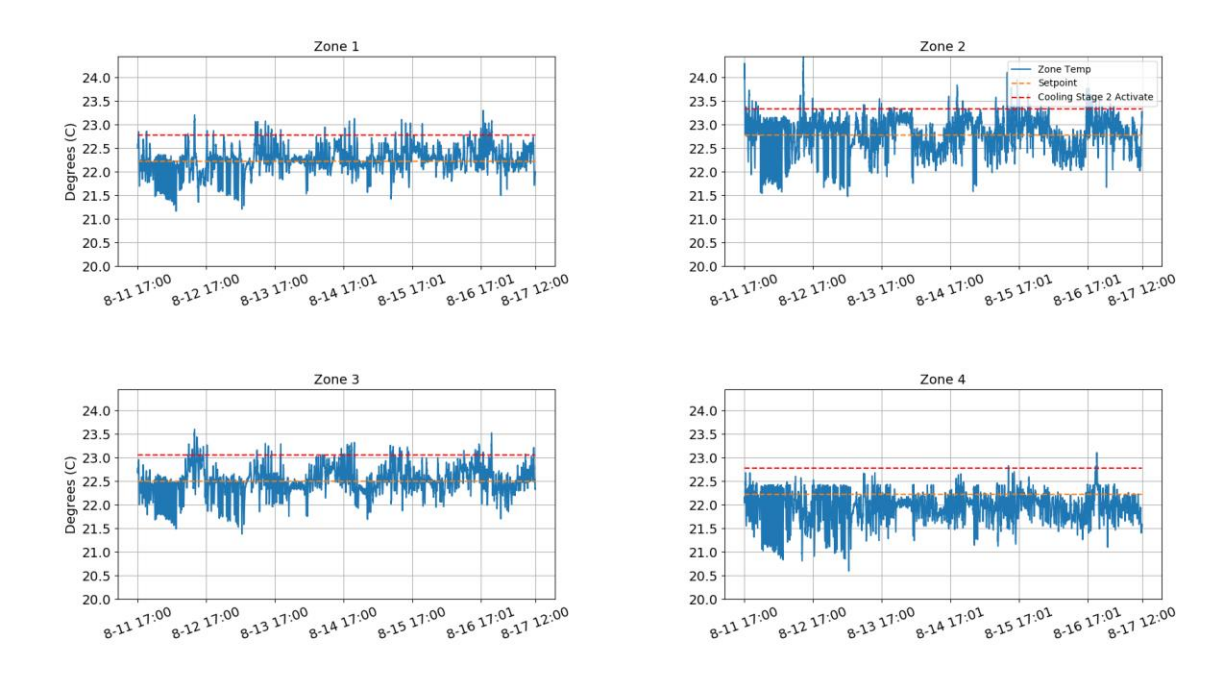


**Fig. 9:** Zone temperatures for controlled week 8/11–8/17.

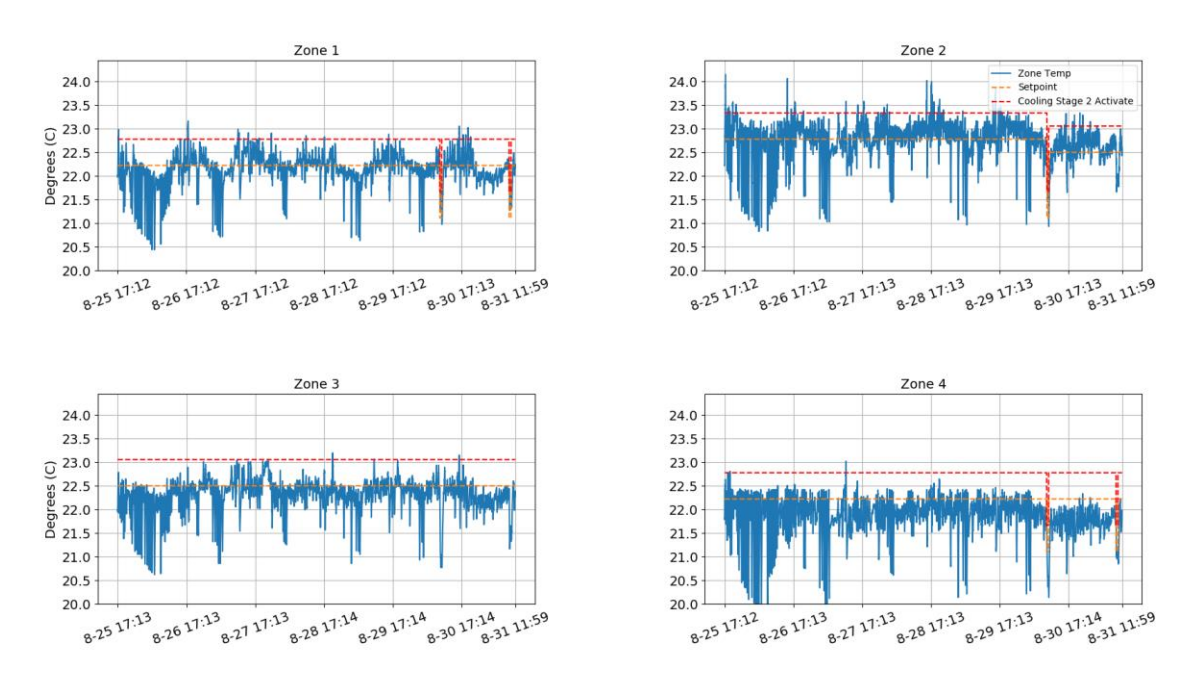
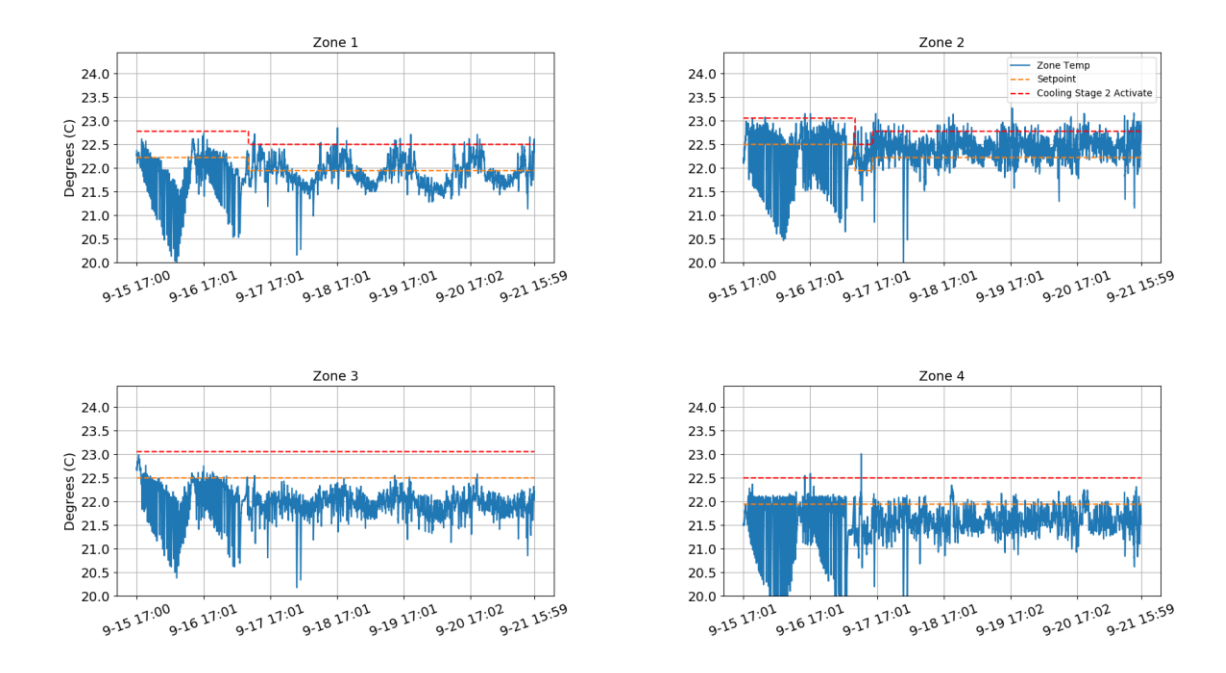


Fig. 10: Zone temperatures for controlled week 8/25–8/31.



**Fig. 11:** Zone temperatures for controlled week 9/15–9/21.

Table 1. Summary of peak demand and ambient conditions.

Week Covered	Peak Demand	Average Maximum	Median Maximum	Total Energy
	(kW)	Temperature (°C)	Temperature (°C)	(kWh)
7/28-8/3	15.85	29.4	28.9	689
(uncontrolled)				
8/18-8/24	17.46	31.1	31.1	770
(uncontrolled)				
8/11-8/17	18.641	33.3	33.9	964
(controlled)				
8/25-8/31	13.34	27.8	28.9	504
(controlled)				
9/15-9/21	12.2	30.0	30.0	541
(controlled)				

While the goal of PBC is to reduce peak consumption, it is important that the total energy consumption is not drastically different from that in the uncontrolled scenario. To demonstrate that this was the case, the total energy consumption was calculated over the experimental period. Table 1 shows that the energy consumption was comparable across similar scenarios and was lower for the controlled cases in the comparison of weeks 7/28–8/3 (uncontrolled) and 8/25–8/31 (controlled), although reducing energy consumption was not the primary objective of the scheduling algorithm. Because energy consumption is correlated with environmental conditions, however, PBC cannot overcome extreme environmental conditions such as the high temperatures in week 8/11–8/17.

## 5. Extending Priority-Based Control

Because peak shaving is a specific case of the more general problem of load shaping, the latter is a natural extension of the PBC algorithm. To that end, a number of modifications were made to the PBC strategy. Priorities were allowed to be negative to allow for precooling when desirable, and the priority band was allowed to float. That is, the algorithm will attempt to meet the load shape under a strict set of comfort constraints but can progressively expand the comfort constraints up to a point, if required. As before, lockout intervals were enforced upon the devices to prevent unacceptably frequent switching. The algorithm was run on 60-second time intervals to allow higher-fidelity control of the load shape.

To ascertain the utility of this load shaping PBC strategy across a large variety of equipment items, the same simulation strategy as before was implemented. That is, the strategy was simulated with 80 HVAC units and 40 refrigeration units. To assess the robustness of the proposed algorithm, the simulation was repeated 3,000 times with a distinct assignment of thermal behavior to each equipment item in each case. This approach led to a simulation set of 360,000

different items of equipment tested in 3,000 distinct combinations. We then examined the deviation from the desired load shape at each time step in each simulation. The load shapes PBC attempted to follow are shown in Fig. 12.

The results of the load-shaping simulations are shown in Fig. 13, which charts the maximum percent deviation from the desired load shape at every time step. That is, at 100% of a reference signal, the load is following the shape perfectly. At 105%, the load is 5% greater, and at 95%, the load is 5% less. Across all of the simulations, the load stayed within 5% of the load shape except for two outliers, in which case there was a spike in the deviation from the set point. A closer look at these outliers is shown in Fig. 14, which shows that these large deviations result from the lag time between when the change in the desired shape is detected and when the algorithm can modulate the demand to follow. This lag is an artifact of PBC's being reactive rather than predictive. Further modification of the algorithm may be necessary to allow for some forward-looking action based on anticipated changes in the desired load shape.

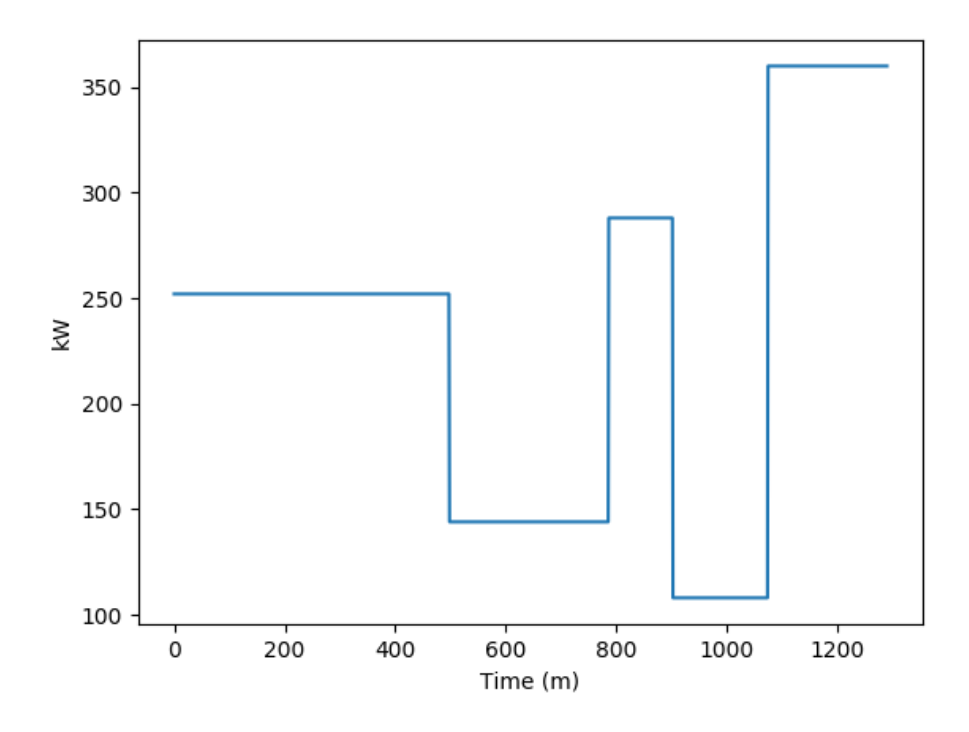
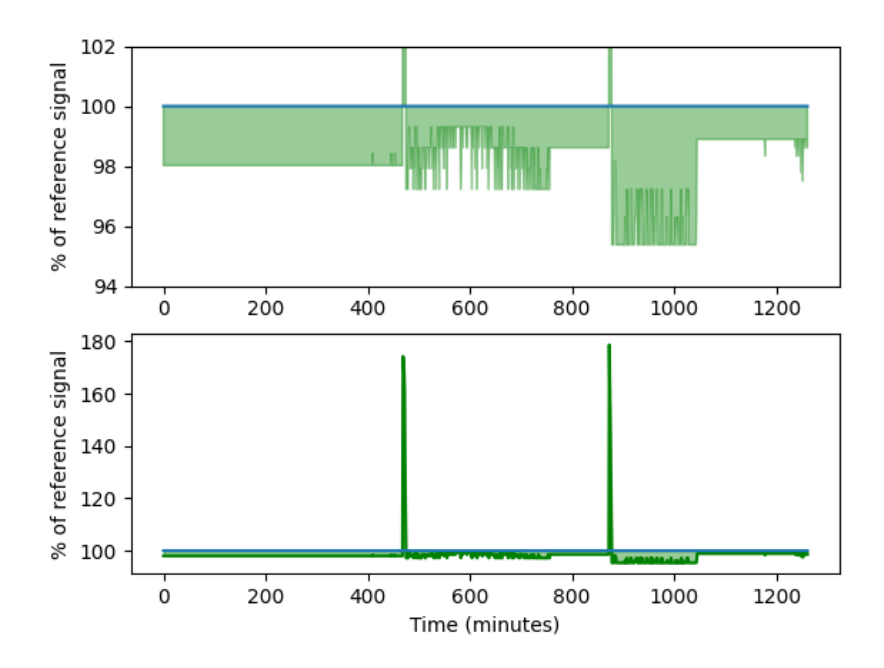


Fig. 12. The load profile that priority-based control seeks to track.



**Fig. 13.** Worst-case deviations from the load shape at each time step across all simulations. The green shaded area represents the deviation from 100% of the desired load shape

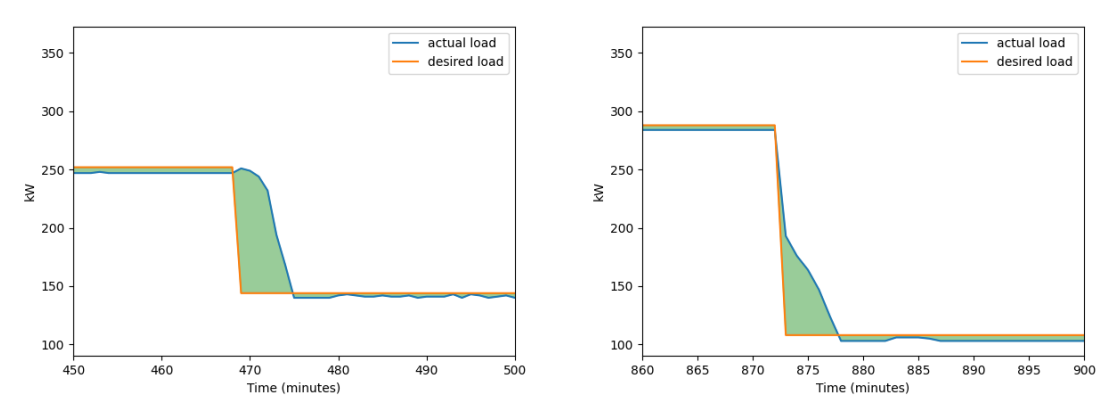


Fig. 14. The two outliers from Fig. 13. These Figures show the actual load shape at the time steps in question.

The green shaded area represents the difference between the two load curves

### 6. Conclusions

This paper presents PBC, an inexpensive control strategy for peak load reduction and load shaping. The computational overhead is drastically reduced compared with the other current strategies, as PBC requires no optimization and the only computation time is that required for list sorting. The developed scheduling strategy was used to simulate 80 HVAC and 40 refrigeration units. The results show that a peak savings of 60 kW can be achieved with significantly fewer devices compared with a traditional set point—deadband approach. The algorithm was deployed in a gymnasium to demonstrate its applicability in a real building, thereby demonstrating the practicality of the proposed approach.

The field test and simulation results present a strong case that PBC offers a viable method for reducing peak demand in HVAC and refrigeration systems used in small commercial buildings. These buildings are typically not under the control of energy management systems and so are prime candidates for the installation of PBC as a retrofit technology. Indeed, given the modest near-term return on peak energy reduction, an inexpensive technology with a commensurately short payback period will be essential for commercial adaptation of any control system. Nevertheless, this modest return for an individual building owner becomes very substantial when energy use is viewed in terms of national or global resources.

We anticipate future demonstrations of the PBC in food sales buildings with a specific focus on refrigeration systems. Additional development is being pursued to support a robust load-shaping capability following earlier developed theoretical guarantees. The simulation results suggest that the strategy as implemented can track a load shape, and they point toward a generic capability to follow curves as is required to provide several grid services.

## Acknowledgements

Funding: This work was funded by field work proposal 3CEBT356 under US Department of Energy Building Technologies Office Activity Number BT0304030.

### References

- [1] F.C. Schweppe, R.D. Tabors, J.L. Kirtley, H.R. Outhred, F.H. Pickel, A.J. Cox, Homeostatic utility control, IEEE Trans. Power Appar. Syst. (1980) 1151–1163.
- [2] D.S. Callaway, I.A. Hiskens, Achieving controllability of electric loads, Proc. IEEE. 99 (2011) 184–199. https://doi.org/10.1109/JPROC.2010.2081652.
- [3] U.S.Energy Information Administration, CBECS (2012), Commercial Buildings Energy Consumption Survey: Energy Usage Summary, (n.d.).
- [4] EIA, The 2012 Commercial Building Energy Consumption Survey, (2016). https://www.eia.gov/consumption/commercial/data/2012/index.php?view=microdata.
- [5] The Cadmus Group, Northwest Commercial Building Stock Assessment, (2009). https://neea.org/img/documents/2009NorthwestCommercialBuildingStockAssessment021 CA220F212.pdf.
- [6] CEC (California Energy Commission), Enhanced Automation Case Study 7: Lighting and Equipment Controls/Grocery Store, (2005). https://www.energy.ca.gov/2005publications/CEC-400-2005-059/CEC-400-2005-059-FS.PDF.
- [7] M. Deru, A. Hirsh, J. Clark, J. Anthony, Field Testing and Modeling of Supermarket Refrigeration Systems as a Demand Response Resource, in: ACEEE Summer Study Energy Effic. Build., 2016: pp. 1–12.
- [8] NREL, A Survey of U.S. Demand Charges, (2017). https://www.nrel.gov/solar/assets/pdfs/2017-us-demand-charges-webinar.pdf.
- [9] X. Hu, J. Nutaro, A Priority-Based Control Strategy and Performance Bound for Aggregated HVAC-Based Load Shaping, IEEE Trans. Smart Grid. (2020).
- [10] D.S. Callaway, Tapping the energy storage potential in electric loads to deliver load following and regulation, with application to wind energy, Energy Convers. Manag. 50 (2009) 1389–1400. https://doi.org/10.1016/j.enconman.2008.12.012.
- [11] S. Kundu, N. Sinitsyn, S. Backhaus, I. Hiskens, Modeling and control of thermostatically controlled loads, (2011). http://arxiv.org/abs/1101.2157.
- [12] H. Hao, B.M. Sanandaji, K. Poolla, T.L. Vincent, A generalized battery model of a collection of thermostatically controlled loads for providing ancillary service, in: 2013 51st Annu. Allert. Conf. Commun. Control. Comput., IEEE, 2013: pp. 551–558.
- [13] S. Koch, J.L. Mathieu, D.S. Callaway, Modeling and Control of Aggregated Heterogeneous Thermostatically Controlled Loads for Ancillary Services Stephan, in: 17th Power Systems Computation Conference, Stockholm Sweden, 2011.
- [14] Y. Bao, On the Accuracy of the State-Queuing Model for the Thermostatically Controlled Loads, 2016 IEEE PES Asia-Pacific Power Energy Eng. Conf. (2016) 1990–1994. https://doi.org/10.1109/APPEEC.2016.7779862.
- [15] Y.-Q. Bao, M. Hu, Y.-Y. Hong, P.-P. Chen, J.-Q. Ju, G. Ma, Accuracy analysis and improvement of the state-queuing model for the thermostatically controlled loads, IET

- Gener. Transm. Distrib. 11 (2017) 1303–1310. https://doi.org/10.1049/iet-gtd.2016.1427.
- [16] S. Esmaeil Zadeh Soudjani, A. Abate, Aggregation of thermostatically controlled loads by formal abstractions, IEEE Trans. Control Syst. Technol. 23 (2015) 4232–4237. https://doi.org/10.23919/ecc.2013.6669547.
- [17] J.L. Mathieu, D.S. Callaway, State estimation and control of heterogeneous thermostatically controlled loads for load following, Proc. Annu. Hawaii Int. Conf. Syst. Sci. (2012) 2002–2011. https://doi.org/10.1109/HICSS.2012.545.
- [18] L.C. Totu, R. Wisniewski, Demand response of thermostatic loads by optimized switching-fraction broadcast, IFAC, 2014. https://doi.org/10.3182/20140824-6-ZA-1003.02439.
- [19] V. Lakshmanan, M. Marinelli, J. Hu, H.W. Bindner, Provision of secondary frequency control via demand response activation on thermostatically controlled loads: Solutions and experiences from Denmark, Appl. Energy. 173 (2016) 470–480. https://doi.org/10.1016/j.apenergy.2016.04.054.
- [20] V. Lakshmanan, M. Marinelli, A.M. Kosek, P.B. Nørgård, H.W. Bindner, Impact of thermostatically controlled loads' demand response activation on aggregated power: A field experiment, Energy. 94 (2016) 705–714. https://doi.org/10.1016/j.energy.2015.11.050.
- [21] V. Lakshmanan, M. Marinelli, A.M. Kosek, Thermostat controlled loads flexibility assessment for enabling load shifting An experimental proof in a low voltage grid, 2017 52nd Int. Univ. Power Eng. Conf. UPEC 2017. 2017-Janua (2017) 1–6. https://doi.org/10.1109/UPEC.2017.8231932.
- [22] Z. Xu, J. Østergaard, M. Togeby, C. Marcus-Møller, Design and modelling of thermostatically controlled loads as frequency controlled reserve, 2007 IEEE Power Eng. Soc. Gen. Meet. PES. (2007) 1–6. https://doi.org/10.1109/PES.2007.386014.
- [23] Y. Zhou, C. Wang, J. Wu, J. Wang, M. Cheng, G. Li, Optimal scheduling of aggregated thermostatically controlled loads with renewable generation in the intraday electricity market, Appl. Energy. 188 (2017) 456–465. https://doi.org/10.1016/j.apenergy.2016.12.008.
- [24] N. Lu, An evaluation of the HVAC load potential for providing load balancing service, IEEE Trans. Smart Grid. 3 (2012) 1263–1270. https://doi.org/10.1109/TSG.2012.2183649.
- [25] N. Lu, Y. Zhang, Design considerations of a centralized load controller using thermostatically controlled appliances for continuous regulation reserves, IEEE Trans. Smart Grid. 4 (2013) 914–921. https://doi.org/10.1109/TSG.2012.2222944.
- [26] H. Hao, B.M. Sanandaji, K. Poolla, T.L. Vincent, Aggregate flexibility of thermostatically controlled loads, IEEE Trans. Power Syst. 30 (2015) 189–198. https://doi.org/10.1109/TPWRS.2014.2328865.
- [27] H.H.M. Weerts, S.E. Shafiei, J. Stoustrup, R. Izadi-Zamanabadi, Model-based predictive control scheme for cost optimization and balancing services for supermarket refrigeration systems, IFAC, 2014. https://doi.org/10.3182/20140824-6-ZA-1003.01056.
- [28] R. Pedersen, J. Schwensen, B. Biegel, J. Stoustrup, T. Green, Aggregation and control of supermarket refrigeration systems in a smart grid, IFAC, 2014. https://doi.org/10.3182/20140824-6-ZA-1003.00268.
- [29] N. O'connell, P. Pinson, H. Madsen, M. O'malley, Economic Dispatch of Demand Response Balancing Through Asymmetric Block Offers, IEEE Trans. Power Syst. 31 (2016) 2999–3007. https://doi.org/10.1109/TPWRS.2015.2475175.
- [30] B. Fricke, T. Kuruganti, J. Nutaro, D. Fugate, J. Sanyal, Utilizing Thermal Mass in Refrigerated Display Cases to Reduce Peak Demand, in: 2016.

- http://docs.lib.purdue.edu/iracc%5Cnhttp://docs.lib.purdue.edu/iracc/1760.
- [31] J. Nutaro, O. Ozmen, J. Sanyal, D. Fugate, T. Kuruganti, Simulation based design and testing of a supervisory controller for reducing peak demand in buildings, in: Int. High Perform. Build. Conf., Purdue, 2016.
- [32] J. Forrest, T. Ralphs, S. Vigerske, LouHafer, K. Bjarni, Jpfasano, coin-or/Cbc: Version 2.9.9 (Version releases/2.9.9). Zenodo., (n.d.). http://doi.org/10.5281/zenodo.1317566.
- [33] Coelho, L.& Laporte, G.& Lindbeck, A.& Vidal, Thibaut, Benchmark Instances and Branch-and-Cut Algorithm for the Hashiwokakero Puzzle, Technical (2019).
- [34] PNNL, VOLTTRON, (2015). http://bgintegration.pnnl.gov/volttron.asp.